

## Membranes of Triphenylsilyl Substituted Polyphenylene Oxide in the Permeation of Propylene and Propane Gases

Susheela Bai Gajbhiye

Department of Engineering Chemistry, College of Engineering, Andhra University, Visakhapatnam 530 003, India

Correspondence to: S. B. Gajbhiye (E-mail: yahuinsb@yahoo.co.in)

**ABSTRACT:** Poly(2,6-dimethyl-1,4-phenylene oxide) (PPO) was chemically modified by the attachment of a bulky triphenylsilyl (TPS) group substituent (~30 mol %) to study its impact on hydrocarbon gas permeation. A membrane of the modified PPO (TPS-PPO) was tested for the permeation of pure propylene and propane gas and that of their 55:45 binary mixture at  $30 \pm 2^\circ\text{C}$ . Gravimetric single-gas equilibrium sorption studies were carried out to determine the gas solubility coefficients and diffusion coefficients to assess their role in the gas permeation mechanism of the membranes. Characterization studies were done to determine the interrelationship between the transport properties and the polymer structure. The studies included density, fractional free volume, Fourier transform infrared spectroscopy,  $^1\text{H-NMR}$ , differential scanning calorimetry, wide-angle X-ray diffraction, tensile testing, and scanning electron microscopy. The TPS-PPO membrane was found to be 3 times more permeable to propylene and 3.8 times more permeable to propane with a small decrease in the propylene/propane ideal permselectivity (3.37) when compared to that of unmodified PPO (4.25). TPS-PPO could be a potential membrane material for the efficient recovery of propylene and propane from mixtures with permanent gases such as those found in refinery off-gas. © 2013 Wiley Periodicals, Inc. *J. Appl. Polym. Sci.* 129: 2464–2471, 2013

**KEYWORDS:** glass transition; membranes; properties and characterization; separation techniques; structure-property relations

Received 22 July 2012; accepted 29 November 2012; published online 30 January 2013

DOI: 10.1002/app.38888

### INTRODUCTION

Rubbery polymers are highly permeable, whereas glassy polymers are highly permselective. Among these two classes of polymers, by experimental studies and theoretical calculations, ethyl cellulose (EC) and poly(2,6-dimethyl-1,4-phenylene oxide) (PPO) polymers have been found to be potential membrane materials in the separation of propylene from propane.<sup>1–3</sup> However, EC membranes exhibited reasonably higher gas permeabilities with typically low selectivities,<sup>1,2</sup> whereas PPO membranes gave relatively lower gas permeabilities and marginally higher propylene/propane permselectivities.<sup>2,3</sup> To prepare a polymer membrane that has a higher gas permeability than EC and a higher permselectivity than PPO, attempts were made to blend PPO and EC. However, the blended membranes showed poor strength because of phase separation. Hence, in this investigation, PPO was modified with triphenylsilyl (TPS) group substitutions to obtain a membrane with permeabilities as high as EC to improve its performance. To overcome the trade-off trend between the gas permeability and the permselectivity of polymer membranes, it is also vital to understand the interrelationship between the polymer molecular structure and its membrane transport mechanism.

PPO is a cost-effective, high performance thermoplastic polymer having a high temperature stability, easy availability, good processability, and excellent stability to hydrolysis. Its molecular structure allows easy substitution at both the benzyl and phenyl positions by various functional groups. Several attempts have been made to improve the gas permeation of PPO by the substitution of various functional groups.<sup>4–6</sup> The introduction of polar functional groups was reported to improve interchain packing and chain rigidity, and this led to low gas permeability and high permselectivity.<sup>7–11</sup> The sulfonation<sup>8</sup> and carboxylation<sup>10</sup> of PPO derivatives were studied, and the effect was observed to be more significant with sulfonated PPO than with carboxylated PPO. Attempts were made to compensate for the loss in permeability of sulfonated PPO by simultaneous bromination.<sup>11</sup> The less polar membranes of brominated PPO were found to be effective in increasing the solubility of  $\text{CO}_2$ ,  $\text{CH}_4$ , and  $\text{N}_2$  with increasing bromination, and this change was prominent for gases with lower condensability.<sup>12</sup> However, the permselectivity exhibited leveling off around 17–20 even at higher degrees of brominations. PPO was also modified by trialkyl- and triaryl-substituted silyl<sup>13</sup> and diphenyl groups.<sup>14–16</sup> Silicone-substituted polystyrene,<sup>17</sup> trimethylsilyl (TMS)-substituted polypropylene,<sup>18</sup> TMS-PPO, and TMS-poly sulfone<sup>19</sup> produced significant enhancements in

permeabilities with insignificant losses in permselectivity. Not only did the nature of the substituent groups impact the membrane gas transport properties, but the symmetry and site of substitution also influenced the molecular structure and, hence, the gas transport. For instance, in TMS-substituted polysulfone, the substitution on the aryl groups near the more mobile ether linkage was found to be more effective in reducing the glass transition and suppressing the interchain packing than that at the sulfone linkage.<sup>20</sup>

On the basis of his studies on bulky group substitutions, Koros et al.<sup>4</sup> proposed a qualitative principle that is accepted by most researchers "if there is suppression of interchain packing on addition of bulky groups and/or kinks in the backbone with simultaneous inhibition of intrachain motion around flexible hinge points, then it tends to increase permeability without unacceptable losses in permselectivity."

Among the bulky group substituents, TMS was found to be very effective in increasing the gas permeability by hindering the segmental mobilities of the main chain and, thereby, disrupting chain packing with enough interchain spacing because of steric bulkiness and higher electrostatic interactions.<sup>13,17,18</sup> When the three methyl groups on silicon were replaced by three rigid phenyl groups (TPS), the resulting polymer exhibited increased segmental mobilities [a decrease in glass-transition temperature ( $T_g$ )] and also increased interchain spacings because of low hindrance to segmental motion of the main chain; this, thereby, enhanced chain packing.<sup>13</sup> Zhang and Hou<sup>13</sup> studied the gas transport behavior of both TMS- and TPS-substituted PPO with specific attention to nonpolar, permanent gases such as  $N_2$ ,  $O_2$ ,  $H_2$ ,  $CH_4$ , and  $CO_2$  (a condensable gas).

In this study, a TPS-substituted PPO membrane was studied in the permeation of  $C_3$  hydrocarbon gases. The modification of PPO polymer was carried out by the introduction of TPS on the methyl groups of the phenylene oxide. Simple lithiation and corresponding silylation was followed with substitution kept at about 30 mol %. The membranes of the polymers were tested for the permeation of pure gas and a binary mixture of propylene and propane. The membranes were also tested for single-gas gravimetric sorption measurements. The polymers were characterized for structure–property interrelationships by density ( $\rho$ ) measurements, fractional free volume (FFV) calculations, Fourier transform infrared (FTIR) spectroscopy, NMR, differential scanning calorimetry (DSC), wide-angle X-ray diffraction (WAXD), tensile testing, and scanning electron microscopy (SEM). The observed transport properties of the membrane for propylene and propane were found to be different on comparison with those of nonpolar permanent gases found by other researchers. The observed differences in the transport behavior of the propylene and propane gases through the modified membrane were attributed to the various specific physicochemical properties analyzed.

## EXPERIMENTAL

### Materials

PPO polymer with a number-average molecular weight of 32,000 and a weight-average molecular weight of 244,000 with a  $\rho$  of 1.06 g/cm<sup>3</sup> at 25°C was purchased from Aldrich Chemical

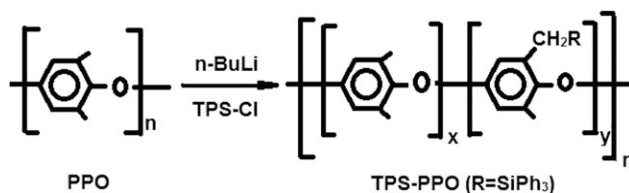


Figure 1. Preparation of TPS-PPO.

Co (Milwaukee, Wisconsin, USA). Its specification  $T_g$  was 211°C, and its melting temperature was 268°C. Chlorotriphenylsilane (TPS-Cl) and  $n$ -butyl lithium ( $n\text{-BuLi}$ ), were procured from E. Merck India, Ltd. (Mumbai, India). Tetrahydrofuran, hexane, methanol, and acetone were of synthesis grade, and they were used without further purification. Propylene and propane gases obtained from Boruka Gas, Ltd. (Bangalore, India) were found to be 99.5% pure and were used without further purification. A gas mixture containing about 45 mol % propane and about 55 mol % propylene was prepared online with the help of multichannel mass flow controllers calibrated with a soap bubble meter. Two mixing vessels were installed in the feed line to ensure the homogeneity of the mixtures.<sup>1</sup>

### Synthesis

TPS-substituted PPO (TPS-PPO) was synthesized by a simple one-step reaction by the lithiation (with  $\text{BuLi}$ ) of PPO followed by treatment with TPS-Cl, as shown in Figure 1. The molar fraction of the TPS group per PPO repeat unit was controlled by the molar content of TPS-Cl. The resulting polymer was precipitated with methanol, and the liquid was removed by filtration. The solid was washed with methanol and acetone, and then, the polymer was dried completely. The polymer so formed was then characterized by various methods.

### Membrane Fabrication

Membranes about 60  $\mu\text{m}$  thick were cast at room temperature on clean, dust-free glass plates by the spreading of a 12 wt % homogeneous chloroform solution of the polymers. The desired thickness of the membrane was controlled by a doctor's blade. The solvent was completely evaporated, and the membranes were stripped off from the glass plate with water as a nonsolvent and were dried further *in vacuo* for 6 h to remove traces of solvent.

### Polymer Characterization

FTIR spectroscopy was performed on the chloroform solution cast thin films of the polymers, which were vacuum-dried. A Shimadzu FTIR instrument (Tokyo, Japan) was used for scanning the films at ambient temperature at a rate of 200 sweeps/s. Proton NMR spectra were obtained on a Gemini 200-MHz machine (New Jersey, USA) with  $\text{CDCl}_3$  as the solvent.

WAXD spectra were obtained with a Siemens D5000 powder X-ray diffractometer (Texas, USA) to find the effective spacing between intersegmental polymer chains, as characterized by  $d$ -spacing ( $d_{\text{eff}}$ ) of the polymers, under conditions similar to those reported earlier.<sup>16</sup> X-rays of wavelength 1.5406 Å were generated with a  $\text{Cu K}\alpha$  source. The  $2\theta$  values were varied from 0 to 65°. The powder samples were partially wetted in toluene vapor (yet retained their powdery nature) and were then used for diffraction

studies to reduce the anisotropy of the diffracting planes. Bragg's equation of first order was used to calculate  $d_{\text{eff}}$  from the  $2\theta$  values of the polymers, which is reported with an accuracy of  $\pm 0.01$ .

Elemental analysis was performed on Vario-EL elemental analyzer (Hanau, Germany). A scanning electron microscope (Hitachi-S 520 model, Tokyo, Japan) was used to study the surface morphology of the polymers. Before analysis, the film sample was coated with a thin layer of gold. Elemental analysis was also carried out with an EDAX system (LINK ISIS-300, Oxford Corp., Dallas, Texas, USA).

The  $\rho$  of the polymer membranes was measured with an accuracy of  $\pm 0.001 \text{ g/cm}^3$  by a floatation method at  $30 \pm 2^\circ\text{C}$  with mixtures of ethylene glycol and DMF solvents. The FFV values of the polymers were estimated with their  $\rho$  values. FFV was defined as  $\text{FFV} = V_f/V_{sp}$ , where  $V_f$  is the free volume and  $V_{sp} = 1/\rho$  is the specific volume of the polymer. According to Bondi's equation,  $V_f$  is estimated as  $V_f = V_{sp} - 1.3 V_w$ , where  $V_w$  is the van der Waal's volume of the repeat unit of the polymer and it is calculated using group contribution method.<sup>21</sup> The FFV values have been reported with an accuracy  $\pm 0.005$ .

Thermal analysis was carried out to find the  $T_g$  of the polymers on PerkinElmer DSC-7 (Connecticut, USA) instrument. The scans were placed in the temperature range of  $25\text{--}300^\circ\text{C}$  at a heating rate of  $10^\circ\text{C}/\text{min}$ .

The mechanical properties such as the tensile strength and percentage elongation at break of the polymer films ( $60 \mu\text{m}$  thick) cut as rectangular pieces were determined with a universal tensile testing machine (AGS-10 KNG, Shimadzu, Tokyo, Japan) at a deformation rate of  $5 \text{ mm}/\text{min}$  with a gage length of  $7 \text{ cm}$ . The average value calculated from five films of each polymer sample are reported.

### Gas Permeation Studies on the In-House Built Gas-Separation Manifold

A schematic of the experimental setup used for the gas permeation studies was demonstrated in our earlier report.<sup>1</sup> The experiments were conducted at a temperature of  $30 \pm 2^\circ\text{C}$  with pure gases and with mixtures of propane (44.9 mol %), propylene (54.95 mol %), and  $\text{C}_2$  hydrocarbon (0.15 mol %). The mixtures were tested on a manifold containing two feed lines connected to two mixing chambers. A continuous flow method was used for the permeation studies. Membranes fabricated from TPS-PPO were mechanically strong enough to withstand the applied feed pressures without undergoing any leakage or rupture.

The experimental procedure was described elsewhere.<sup>1,16</sup> The respective pure and mixture gas permeabilities, propylene/propane ideal permselectivity ( $\alpha_{\text{ideal}}$ ), and permselectivity for the binary mixture ( $\alpha_{\text{mix}}$ ) were calculated and are reported as overall averages with an error margin of less than 3.0%.

The permeability coefficient ( $P$ ) of a gas, reported in Barrers, was calculated as follows:

$$P(\text{Barrer}) = J \times l/\Delta p \quad (1)$$

where  $J$  is flux of the permeating gas [ $\text{cm}^3$  (STP)  $\text{s}^{-1} \text{ cm}^{-2}$ ],  $l$  is thickness of the membrane (cm), and  $\Delta p$  is the partial pressure

difference between the feed and permeate side (cmHg;  $1 \text{ cmHg} = 1.33 \times 10^3 \text{ Pa}$ ).  $\alpha_{\text{ideal}}$  of the membrane was determined as the ratio of the  $P$  values of the two gases:

$$\alpha_{\text{ideal}} = P_{(\text{C}_3\text{H}_6)}/P_{(\text{C}_3\text{H}_8)} \quad (2)$$

The mixture gas permselectivity was calculated as follows:

$$\alpha_{\text{mix}} = y(1-x)/x(1-y) \quad (3)$$

where  $y$  is the composition of propylene in the permeate and  $x$  is the composition of propylene in the feed.

### Gravimetric Sorption Experiments

The solubility and diffusivity coefficients of the polymer films were determined by a gravimetric method with single-gas equilibrium sorption studies carried out on a Cahn D200 electrobalance (Cahn Instruments, Cerritos, CA) with a sensitivity of  $10^{-7} \text{ g}$  and a precision of  $5 \times 10^{-6}$ . The balance was maintained in a constant-temperature chamber ( $30 \pm 2^\circ\text{C}$ ).

The balance was initially calibrated with a known weight. An inert gas stream was allowed to flow through the sample cell as a first step to remove traces of volatile matter. Polymer film samples of a constant thickness ( $100 \text{ mg}$ ), vacuum-dried at  $60^\circ\text{C}$  until constant weight, were suspended from one arm of the electrobalance, and a constant concentration of the sorbate gas (propylene and propane) was continuously flowed through the sample cell tube, such that the sample film was totally surrounded by the gas. The concentration of the gas was maintained throughout the experiment by mixture with a pure nitrogen gas stream. Both gases were maintained at controlled flow rates with the help of soap bubble meters and a precision needle valve. A buoyancy effect at the range of flow rates used in this study was avoided with a large distance between the sample and the stream entrance and a large expansion section, which reduced the linear flow of the gas through the sorption cell. Data were collected by an interfaced computer program, from time  $t = 0$  to the time at which the film sample showed a constant weight. Sorption experiments were carried out at a gas pressure of 0.8 bars with propylene and propane. Higher pressure sorption tests were not conducted to eliminate any plasticization effects. The experiments were repeated three times, and the results are reported with an error margin of less than 2.0%

From the sorbate uptake graphs, the solubility coefficient ( $S$ ) was calculated with the following equation:<sup>22,23</sup>

$$S = w_s/p_s = [m_p(\infty) - m_p(0)]/[m_p(0)] \times [M_s/c_sRT] \quad (4)$$

where  $w_s$  is the sorbate uptake by the polymer,  $p_s$  is the partial pressure of the sorbate gas,  $c_s$  is the sorbate concentration in the gas phase,  $M_s$  is the molecular mass of the sorbate,  $R$  is the gas constant,  $T$  is the temperature (K), and  $m_p(0)$  and  $m_p(\infty)$  are the polymer masses before sorption and after equilibrium sorption, respectively.

The diffusion coefficient ( $D$ ) was obtained from the time at which sorption by the film reached 50% of its total extent ( $t_{1/2}$ ) with the following equation:<sup>22,23</sup>

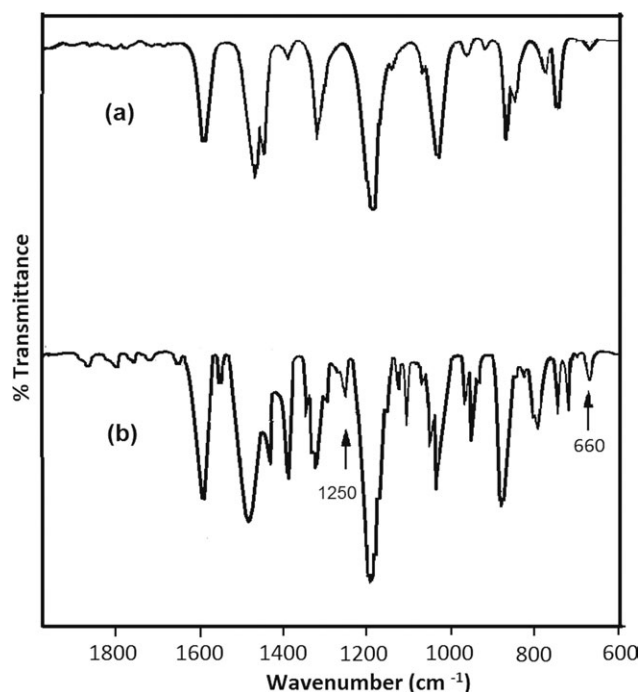


**Figure 2.** FTIR spectra of the fingerprint region of (a) PPO and (b) TPS-PPO.

$$D = 0.0492 l^2 / t_{1/2} \quad (5)$$

## RESULTS AND DISCUSSION

### Polymer Characterization

PPO and TPS-PPO were characterized according to their physicochemical properties by various instrumental methods.

**FTIR Spectra.** The FTIR spectra of the fingerprint TPS-PPO and PPO are shown in Figure 2. PPO exhibited methyl group deformations at 1380, 1141, and 1116  $\text{cm}^{-1}$ . Aromatic C=C stretching appear as a strong band at 1490–1425  $\text{cm}^{-1}$  and as a sharp peak at 1606  $\text{cm}^{-1}$ . The absorptions at 1306 and 1022  $\text{cm}^{-1}$  were the C—O—C (ether) group stretching vibrations, and their characteristic deformations occurred at 1185–1200  $\text{cm}^{-1}$ . The FTIR spectra of the TPS-PPO exhibited characteristic medium bands for Si—C<sub>6</sub>H<sub>5</sub> bond stretching vibrations around 1430 and 1100  $\text{cm}^{-1}$ ; for Si—CH<sub>2</sub> stretching vibrations around 1250  $\text{cm}^{-1}$  and a small absorption peak for C—Si stretching at 660  $\text{cm}^{-1}$ .<sup>24</sup> Thus, the presence of about 30 mol % TPS substituted on the methyl group could be confirmed with the fingerprint region absorptions at 1250  $\text{cm}^{-1}$ . At low degrees of bulky group (TPS) substitutions on the less sterically hindered positions, the lateral methyl positions were predominantly occupied.<sup>13</sup> Researchers experimentally proved that at less than 40 mol % of substitution, the TPS group predominantly occupies methyl position of PPO.<sup>13</sup> However, at higher degrees of substitution, occupancy at the backbone phenylene ring position is also possible. Thus, at 30 mol %, TPS substitution could be inferred to be predominant on the methyl groups.

**Proton NMR Spectra.** For PPO, a six-proton singlet corresponding to two equivalent methyl protons was observed at  $\delta = 2.1$  ppm, and the remaining two equivalent aromatic protons gave a two-proton singlet absorption at  $\delta = 6.4$  ppm. The proton NMR of the triphenylsilyl (TPS)-substituted PPO exhibited the following characteristic peaks: a singlet at  $\delta = 2.4$  ppm for methyl and methylene protons and a multiplet at  $\delta = 6.8$ –7.8 ppm corresponding to phenylene and —SiPh together.<sup>24</sup> The molar substitution of TPS groups was calculated to be 30 mol % with elemental analysis, as the NMR method could not be used to determine the percentage of substitution because of the merged multiplet peaks of —SiPh and —Ph group protons.

**T<sub>g</sub>.** The DSC picture is shown in Figure 3. T<sub>g</sub> of PPO at 215°C decreased to 208°C upon incorporation with 30 mol % TPS groups (Table I). In the case of bulky group substitutions, the polymers with symmetrically attached groups or with groups directly attached on the phenylene rings bound to flexible (etherlike) linkages showed increases in T<sub>g</sub> because of hindrances to the main-chain segmental mobility,<sup>16</sup> whereas T<sub>g</sub> decreased when the substitutions were made asymmetrically.<sup>19</sup> Further, from a research study on the molecular conformations of triphenylsilane (TPS—H), the bond length of Si—C bond was established to increase with the number of phenyl groups on the Si atom.<sup>25</sup> Hence, because of the longer Si—C bonds of the TPS side chains when attached asymmetrically at the methyl groups of PPO, the three rigid phenyl groups of TPS caused no steric hindrance to the main-chain segmental motion; this, thereby, lowered the T<sub>g</sub> of the polymer. Additionally, at a low 30 mol % substitution of TPS, the attachments were confirmed to be on the methyl groups of PPO because of the bulky nature of the three phenyl groups of the TPS moiety and not directly on the phenyl ring positions owing to the steric effects.

**$\rho$ .** The measured  $\rho$  of PPO was 1.050  $\text{g}/\text{cm}^3$  and increased to 1.089  $\text{g}/\text{cm}^3$  for the TPS-PPO membrane (Table I). The increase in  $\rho$  indicated that the polymer chain packing was improved on the addition of the TPS groups on the methyl group. The longer Si—C bonds in TPS groups in the side chain possibly reduced

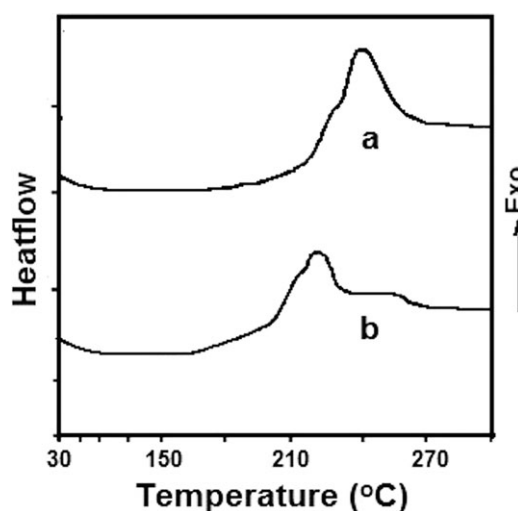


**Figure 3.** DSC pictures of (a) PPO and (b) TPS-PPO.



**Table I.** Physical and Mechanical Properties of the PPO and TPS–PPO Membranes

Polymer	$\rho$ (g/cm <sup>3</sup> )	$V_w$ (cm <sup>3</sup> /g)	$V_f$ (cm <sup>3</sup> /g)	FFV	$T_g$ (°C)	Tensile strength (MPa)	Elongation at break (%)
PPO	1.050	0.6119	0.157	0.1659	215	55.9	17.5
TPS–PPO	1.089	0.6038	0.133	0.1451	208	80.2	25.3

the hindrance caused by the side chain to the segmental movements of the main chain of PPO. The larger segmental movements gave rise to conformational freedom to the polymer chains to pack efficiently.

**FFV.** FFV is an indication of the available volume in the form of voids in the polymer matrix for gas permeation. PPO had a higher FFV value of 0.1659, whereas the TPS–PPO had a reduced FFV of 0.1451 (Table I). This indicated that the size of voids decreased upon modification with TPS groups. This was also interpreted by  $V_f$ , the polymer free volume. The decrease in the free volume  $V_f$  of PPO from 0.157 to 0.133 cm<sup>3</sup>/g after substitution could have been due to the better chain packing caused by TPS groups as explained in the previous section. Consequently, the space available for gas molecules to diffuse was reduced.

**WAXD Results.** Compared to PPO, the diffraction patterns of the TPS–PPO polymer exhibited a less crystalline nature; this indicated that the substitution of TPS groups resulted in a decrease in the crystallinity of the polymer (Figure 4). The diffraction pattern of PPO exhibited characteristic peaks at  $2\theta = 8.0, 12.5, 16.5,$  and  $21.8^\circ$  with the highest peak at  $2\theta = 12.5^\circ$ ; this corresponded to a  $d$ -spacing of 7.07 Å. This implied that the PPO polymer matrix exhibited a range of interchain spacing values with a maximum contribution from the characteristic  $2\theta = 12.5^\circ$  peak corresponding to the dimethyl phenylene unit, whereas TPS–PPO was found to exhibit characteristic peaks at  $2\theta = 7.2, 12.0, 12.8, 15.0,$  and  $21.2^\circ$  with two maxima at  $2\theta$  values of  $12.0$  and  $12.8^\circ$  very closely spaced and corresponding to  $d$ -spacing values of 7.36 and 6.91 Å. This implied that there was a rearrangement of chain segments of PPO upon TPS group incorporation so that the resulting polymer matrix also exhibited the interchain spacing contributions made by the TPS units at  $2\theta = 12.0^\circ$ .

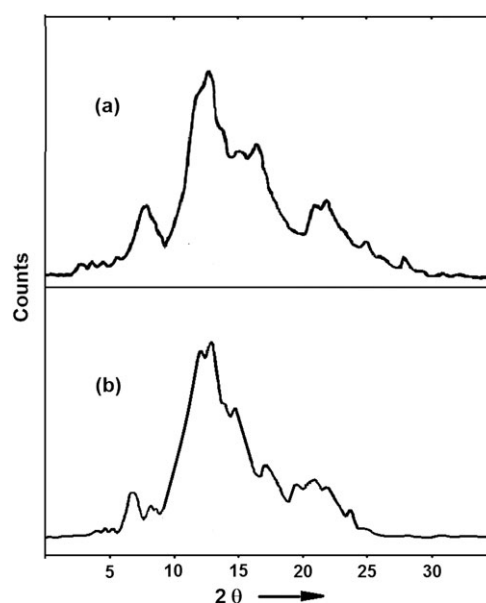
**SEM.** The prepared TPS–PPO membranes were clear and transparent with good mechanical strength. The SEM micrographs indicated homogeneous surface morphology and implied that the TPS–PPO formed a good membrane material.

**Mechanical Properties.** The films of the TPS–PPO polymer exhibited an enhanced tensile strength of 80.2 MPa and an elongation at break of 25.6%, which was higher than that of PPO (Table I).

**Gas Permeation.** The TPS–PPO membrane exhibited increased propylene and propane  $P$  values of 27 and 8 Barrers, respectively, with a minor loss in the propylene/propane  $\alpha_{\text{ideal}}$  (Table II). The  $\alpha_{\text{ideal}}$  of the TPS–PPO membrane decreased to 3.37 in comparison to 4.25 for PPO. The results indicate that TPS groups were effective in increasing the permeability of the

hydrocarbon gases studied. The gas permeation in dense glassy membranes can be well described by the solution–diffusion model, which is governed by two important factors: first, the interaction factors that controlled the solubility (solution) of gas in the membrane, namely, the (1) condensability of the gas molecules and (2) forces of gas–polymer interactions, and second, the structural factors that controlled the gas diffusion, namely, the (1) bulkiness and site of substitution of bulky (TPS) groups, (2) polymer segmental chain mobility, (3) polymer chain packing, (4) dimensions of gas molecules, (5) shape (stereochemical conformations or geometry) of the gas molecules and polymer matrix, and (6) transient interchain channels of the polymer matrix constituting the free volume.

PPO is a semicrystalline polymer with flexible ether links and methyl-substituted rigid aromatic rings. From characterization studies, the substitution of bulky TPS groups on the methyl groups in PPO was observed to change the molecular structural characteristics by lowering the  $T_g$  and by increasing the chain packing (as indicated by a decrease in the free volume). These molecular changes in TPS–PPO generally result in a lowering of the diffusional transport of gases, accompanied by a simultaneous increase in the ideal gas diffusivity–selectivity ( $\alpha_{D,\text{ideal}}$ ). However, in contrast, there was a threefold improvement in the gas permeabilities of TPS–PPO over that of PPO, with a minor lowering in the overall permselectivity. Thus, this implied that there were some other factors that were responsible. In the following sections, a detailed analysis of the (1) interaction factors

**Figure 4.** WAXD patterns of (a) PPO and (b) TPS–PPO.

**Table II.** Pure and Binary Mixture Gas Permeation Results of Propylene and Propane at  $30 \pm 2^\circ\text{C}$  and Feed Pressure of 3 bars

Polymer	$P$ (Barrer) <sup>a</sup>				Permselectivity	
	Propylene		Propane		$\alpha_{\text{ideal}}$	$\alpha_{\text{mix}}$
	Pure	Mixture	Pure	Mixture		
PPO	9.0	6.0	2.1	1.7	4.25	3.5
TPS-PPO	27.0	24.5	8.0	7.7	3.37	3.2

<sup>a</sup>1 Barrer =  $10^{-10}$  [cm<sup>3</sup> (STP) cm cm<sup>-2</sup> s<sup>-1</sup> cmHg<sup>-1</sup>].

and (2) diffusion factors gives an account of the enhancement in permeability and the minor decrease in the ideal selectivity for the TPS-PPO membrane.

**Permeability Enhancement.** From an earlier study (Table III) by Zhang and Hou,<sup>13</sup> the TPS-PPO membrane showed a higher permeability for CO<sub>2</sub> than for CH<sub>4</sub>, although they had similar molecular sizes (Table IV). This indicated that the membrane had a higher affinity for condensable gases and improved the sorption of CO<sub>2</sub> gas. Condensability is generally measured by the normal boiling point, critical temperature, or Lennard-Jones force constant ( $\epsilon/\kappa$ ) of gases. It was also evident that in relation to PPO, the enhancement factors in the gas permeability of the TPS-PPO membrane for the various gases followed the order C<sub>3</sub>H<sub>8</sub> (3.8 times) > C<sub>3</sub>H<sub>6</sub> (3.0 times) > CO<sub>2</sub> (0.98 times) > CH<sub>4</sub> (0.94 times) (Table III). This indicated that the TPS-PPO membrane had not shown any improvement in the permeabilities of the CO<sub>2</sub> and CH<sub>4</sub> gases, whereas a relatively greater affinity was exhibited toward the larger sized propylene and propane gases. This could be attributed to the (1) relatively higher condensability of propylene and propane gases and (2) apparently stronger electrostatic forces of interaction between the hydrocarbon gases and the TPS substituents in TPS-PPO membrane resulting in their greater sorption.

Propylene (because of the presence of double bonds) can have strong  $\pi$ -electron interactions with the additional  $\pi$  electron of the three phenyl groups in the TPS side chains of TPS-PPO, whereas dispersive interactions prevail selectively between sp<sup>3</sup>-hybridized propane and sp<sup>3</sup>-hybridized Si atoms in the TPS side chains of TPS-PPO. Also, propane has a relatively higher condensability than propylene (Table IV). Thus, both gases com-

peted in terms of improving their respective gas solubilities in the TPS-PPO membrane and ultimately contributed toward a higher permeability enhancement factor by over three times.

Additionally, we also found that in comparison to propylene (the unsaturated hydrocarbon), propane (the saturated homologue) was much more selectively permeated by the TPS-PPO membrane, as shown by the permeability enhancement factor of 3.8 for propane (Table III). This could be attributed to an apparent favorable diffusion factor for propane in addition to the solubility factors, as discussed previously. Although propylene, being relatively smaller (Table IV), diffused faster than propane, the latter also appeared to diffuse better than propylene through the TPS-PPO matrix on account of its geometrical conformation tending to be relatively compatible with that of the TPS-PPO polymer;<sup>25</sup> this, thereby, contributed toward its improved permeabilities. The geometry of the TPS groups and its compatibility with that of the propane molecule is elaborated in the following section.

**Geometry of the TPS-PPO and gases.** From a stereochemical point of view, propane has a bent structure because of sp<sup>3</sup> hybridization, whereas propylene has a rigid flat structure due to sp<sup>2</sup> hybridization. Further, from a detailed conformational analysis on triphenylsilane by Campanelli et al.,<sup>25</sup> it was confirmed that the (1) formation of a planar structure was difficult for TPS groups as silicon formed sp<sup>3</sup>-hybridized tetrahedral  $\sigma$  bonds, (2) the three rigid phenyls on the Si atoms offered a twisted, three-blade propeller shape to the TPS group with the phenyl rings twisted at angle of 39°, and (3) from the low-frequency vibrational modes, it was proven that the three phenyl groups undergo large amplitude torsional and out-of-plane bending vibrations about their respective Si-C bonds.<sup>25</sup>

**Mechanism of propane transport through the TPS-PPO membrane.** It is highly possible that when a propeller-shaped

**Table III.** Comparison between the Pure Gas Permeabilities of the PPO and TPS-PPO Membranes and Permeability Enhancement Factors for Various Gases

Gas	Polymer $P$ (Barrer)		Permeability enhancement factor <sup>a</sup>	Reference
	PPO	TPS-PPO		
CH <sub>4</sub>	2.68	2.54	0.94	13
CO <sub>2</sub>	49.2	48.6	0.98	13
C <sub>3</sub> H <sub>6</sub>	9.0	27.0	3.0	This study
C <sub>3</sub> H <sub>8</sub>	2.1	8.0	3.8	This study

<sup>a</sup>Ratio of  $P_{\text{TPS-PPO}}$  to  $P_{\text{PPO}}$ .

**Table IV.** Physical Properties of the Gases

Gas	Boiling point (K)	$\epsilon/\kappa$ (K)	$\sigma_{\text{LJ}}$ (Å) <sup>a</sup>
O <sub>2</sub>	90.2	113	3.48
N <sub>2</sub>	77.4	91.5	3.68
CO <sub>2</sub>	216.6	244	3.30
CH <sub>4</sub>	111.7	137	3.82
C <sub>3</sub> H <sub>6</sub>	225.5	303	4.68
C <sub>3</sub> H <sub>8</sub>	231.1	254	5.03

<sup>a</sup> $\sigma_{\text{LJ}}$ , molecular collision diameter calculated from the Lennard-Jones potential,  $\epsilon/\kappa$ .<sup>26</sup>

TPS side chain, containing three phenyls with large amplitude rotations, is attached to PPO via the methyl groups as the connector, it tends to create small transient microvoids or microchannels. These microchannels, upon local cooperative movements of polymer chains (because of increased chain mobility evident from a decrease in  $T_g$  of TPS–PPO), form continuous nonplanar and bent-shaped transient interchain channels (which constitute the free volume) in the polymer matrix.

Gas transport through dense membranes is a process in which the gas molecules pass along the transient interchain channels, which are invariably different from the micropores present in molecular sieving membranes. Pace and Datyner<sup>27</sup> proposed that the gas-permeation process in glassy solution–diffusion membranes occurs by the movement of gas molecules through a polymer matrix in two distinct ways: (1) sliding longitudinally along interchain channels or (2) jumping or hopping from one interchain channel to other channel whenever adjacent polymer chains are sufficiently separated.<sup>27</sup>

It thus follows that during gas permeation through the TPS–PPO membrane, the rigid and flat-shaped propylene gas molecules upon sorption via  $\pi$ -electron interactions rather diffused out of the transient interchain channels because of a smaller size, whereas the more condensable, flexible, and bent-shaped propane gas molecules, subsequent to greater sorption via a dispersive type of electrostatic interactions with the TPS groups, were able to easily slide through the geometrically favorable transient interchain channels formed under the experimental conditions. Thus, the diffusion of propane was improved in TPS–PPO compared to PPO.

**Ideal selectivity from the sorption studies.** In general, a large increase in the gas permeability of a membrane is always accompanied by a large drop in the permselectivity as per the trade-off. However, for the TPS–PPO membrane, despite a large increase in the gas permeability, a minor decrease in the propylene/propane permselectivity ( $\alpha_{ideal}$ ) of 3.37 was observed against an  $\alpha_{ideal}$  of 4.25 for PPO. This could be explained with the experimental single-gas equilibrium sorption results conducted below an atmospheric pressure of 0.8 bars (Table V). The overall  $\alpha_{ideal}$  of a membrane toward a gas pair is the product of the ideal solubility–selectivity ( $\alpha_{S,ideal}$ ) and  $\alpha_{D,ideal}$ . Further, it has been well established that in dense membranes of PPO, the sorption of a permeant occurs in the polymer matrix via chemical interactions, whereas its diffusion occurs through the interconnected microchannels, which collectively constitute the polymer free volume.<sup>28</sup> Thus, sorption is governed by the compatibility between the functional groups of the permeants and the polymer, whereas diffusion is controlled by the geometrical compatibility (size and/or shape) of the permeating gases with that of the microchannels of the polymer free volume.

**Ideal selectivity of the PPO membrane.** The marginally higher propylene/propane  $\alpha_{ideal}$  of the PPO membrane was a result of contributions majorly from propylene toward the two important factors: (1) propylene/propane  $\alpha_{S,ideal}$  of 0.92 and (2)  $\alpha_{D,ideal}$  of 3.76 (Table V). Factor 1 was attributed to PPO having phenylene groups with clouds of  $\pi$  electrons, which were chemically more compatible with the  $\pi$  electrons of the  $sp^2$ -hybridized propylene molecules. Thus, propylene had better  $\pi$ -electron electrostatic

**Table V.**  $D$ ,  $S$ ,  $\alpha_{D,ideal}$  and  $\alpha_{S,ideal}$  Values in the Membranes of PPO and TPS–PPO for Propylene and Propane Gases at 0.8 bars and  $30 \pm 2^\circ\text{C}$

Polymer (permeant)	$D^a$	$S^b$	$\alpha_{D,ideal}^c$	$\alpha_{S,ideal}^d$
PPO ( $\text{C}_3\text{H}_6$ )	20.01	0.55	3.76	0.92
PPO ( $\text{C}_3\text{H}_8$ )	5.31	0.60		
TPS–PPO ( $\text{C}_3\text{H}_6$ )	19.10	1.76	3.29	0.89
TPS–PPO ( $\text{C}_3\text{H}_8$ )	5.80	1.98		

<sup>a</sup>Unit:  $10^{-10} \text{ cm}^2/\text{s}$ .

<sup>b</sup>Unit:  $[\text{cm}^3 (\text{STP}) \text{ cm}^{-3} \text{ cmHg}^{-1}]$ .

<sup>c</sup> $\alpha_{D,ideal} = D_{\text{C}_3\text{H}_6}/D_{\text{C}_3\text{H}_8}$ .

<sup>d</sup> $\alpha_{S,ideal} = S_{\text{C}_3\text{H}_6}/S_{\text{C}_3\text{H}_8}$ .

interactions with PPO and, hence, selectively sorbed propylene. However, propane, being highly condensable, also got sorbed in PPO to a considerable extent and brought the ratio of the solubilities of the gases closer to 1. Factor 2 was due to the microchannels constituting the free volume in PPO, which tended to be geometrically flat. They were also more rigid because of the presence of rigid phenylene groups in the main chain (high  $T_g$  of PPO) and, thus, could selectively allow the flat-shaped and smaller sized propylene gas to diffuse. Thus, propylene diffused faster relative to the larger and bent-shaped propane in PPO.

**Ideal selectivity of the TPS–PPO membrane.** In the case of the TPS–PPO membrane, the propylene/propane  $\alpha_{ideal}$  was slightly lowered (relative to PPO); this was the outcome of lowered values of the two factors: (1)  $\alpha_{S,ideal}$  of 0.89 and (2)  $\alpha_{D,ideal}$  of 3.29 (Table V). This was due to the contributions from both of the gases, which together participated competitively toward greater sorption and greater diffusion.

The lowering in factor 1, that is,  $\alpha_{S,ideal}$  for TPS–PPO could be attributed to the higher affinity of the TPS–PPO membrane for both the gases because of (1) the competitively better sorption by the condensable propylene via  $\pi$ -electron electrostatic interactions (relative to propane) with the phenyl groups present in TPS–PPO membrane [ $S_{\text{TPS,C}_3\text{H}_6} = 1.76 \text{ cm}^3 (\text{STP}) \text{ cm}^{-3} \text{ cmHg}^{-1}$ ] and (2) a selectively improved propane sorption (relative to propylene) because of its higher condensability (relative to propylene) and a fairly better electrostatic interaction with the  $sp^3$ -hybridized TPS groups of the TPS–PPO polymer [ $S_{\text{TPS,C}_3\text{H}_8} = 1.98 \text{ cm}^3 (\text{STP}) \text{ cm}^{-3} \text{ cmHg}^{-1}$ ].

The lowering in factor 2, that is,  $\alpha_{D,ideal}$  for TPS–PPO could be attributed to (1) the size-based selective diffusion of the smaller sized propylene relative to propane [ $D_{\text{propylene}} = 19.1 \text{ cm}^2/\text{s}$ ] because of the decrease in the free volume of the polymer and (2) that a selectively good sorption of propane due to favorable interactions facilitated its better diffusion through the geometrically compatible interchain channels of TPS–PPO relative to propylene [ $D_{\text{TPS,C}_3\text{H}_8} = 5.8 \text{ cm}^2/\text{s}$ ]. Thus, the two factors together tended to reduce  $\alpha_{D,ideal}$ . The net effect was that the competitive sorption and diffusion of the two gases in TPS–PPO restricted the anticipated large drop in the overall propylene/propane  $\alpha_{ideal}$  to a minor extent.

Thus, with suitable modification of the PPO membranes, it was possible to break the trade-off and get a significant multifold

increase in the permeability with a minor drop in the propylene/propane permselectivity for the hydrocarbon gas separation.

## CONCLUSIONS

This study revealed that a PPO membrane with bulky-group substitutions in the form of TPS–PPO with nearly 30 mol % substitutions was effective in increasing permeability for propylene and propane gases. Relative to the PPO membrane, the TPS–PPO membrane exhibited significantly enhanced gas permeabilities by almost 3.0 times for propylene and 3.8 times for propane; this was accompanied by a minor loss in the overall propylene/propane permselectivity.

From structural characterizations, it was found that TPS group substitutions on PPO led to increased chain packing, a decrease in  $T_g$ , and also a decrease in the polymer free volume because of the bulkiness and the site of substitution of TPS groups on PPO.

The observed significant jump in the permeabilities for propylene and, particularly, for propane in the TPS–PPO membrane compared to PPO was attributed mainly to the higher affinity of the membrane selectively for condensable hydrocarbon gases and the strong electrostatic forces of interaction between the TPS groups and the hydrocarbon gases. In addition, the TPS groups on the PPO chains apparently offered a relatively compatible geometrical conformation for the  $sp^3$ -hybridized less rigid and nonplanar propane molecules to slide through the transient TPS–PPO membrane channels with ease compared to the rigid and flat-shaped propylene molecules; this, thereby, improved the diffusion of propane in particular. Therefore, we found a greater permeability enhancement for propane. Furthermore, the observed minor decrease in the overall propylene/propane permselectivity of TPS–PPO was due to the better sorption and diffusion of both propylene and propane gases in the membrane, with a possible greater contribution from propane.

The study also indicated that the substitution of bulky groups in the polymer backbone, which simultaneously increased the interchain packing and intrachain motion around flexible hinge points, tended to increase the permeability with an acceptable minor loss in permselectivity.

The study also proved that any polymer modified with various functional groups could also be studied for their stereochemical geometries and conformations and their compatibilities with that of the permeating gases to provide deeper insight into the mechanism of gas transport and structure–property correlations.

With the view of the potential of the modified membrane toward hydrocarbons, it is further suggested that their carbonized versions would exhibit promising performance toward the recovery of valuable hydrocarbons from multicomponent mixtures, such as refinery off-gas.

## ACKNOWLEDGMENTS

The support and cooperation provided by S. Sridhar and A. A. Khan of Indian Institute of Chemical Technology, Hyderabad, India, are gratefully acknowledged. The author is also thankful to Hindustan Petroleum Corporation Limited, Visakhapatnam, India,

for sponsoring this project and to the Council of Scientific and Industrial Research, New Delhi, India, for a research fellowship.

## REFERENCES

- Bai, S.; Sridhar, S.; Khan, A. A. *J. Membr. Sci.* **2000**, *67*, 174.
- Sridhar, S.; Bai, S.; Khan, A. A. *J. Polym. Mater.* **2002**, *19*, 133.
- Bai, S.; Sridhar, S.; Khan, A. A. *J. Membr. Sci.* **1998**, *147*, 131.
- Koros, W. J.; Fleming, G. K.; Jordan, S. M.; Kim, T. H.; Hoehn, H. H. *Prog. Polym. Sci.* **1988**, *13*, 339.
- Chern, R. T.; Sheu, F. R.; Jia, L.; Stannett, V. T.; Hopfenberg, H. B. *J. Membr. Sci.* **1987**, *35*, 103.
- Ghosal, K.; Chern, R. T. *J. Membr. Sci.* **1992**, *72*, 91.
- Fu, H.; Jia, L.; Xu, J. *J. Appl. Polym. Sci.* **1994**, *51*, 1405.
- Storey, B.; Koros, W. J. *J. Membr. Sci.* **1992**, *67*, 191.
- Kruczek, B.; Matsuura, T. *J. Membr. Sci.* **1998**, *146*, 263.
- Percec, S.; Li, G. Chemical Modification of PPO and Properties of the Resulting Polymers; ACS Symposium Series 364; American Chemical Society: Washington, DC, **1988**; p 46.
- Hamad, F.; Matsuura, T. *J. Membr. Sci.* **2005**, *253*, 183.
- Percec, S. *J. Appl. Polym. Sci.* **1988**, *36*, 415.
- Zhang, J.; Hou, X. *J. Membr. Sci.* **1994**, *97*, 275.
- Ilinich, O. M.; Semin, G. L.; Chertova, M. V.; Zamarev, K. J. *J. Membr. Sci.* **1992**, *66*, 1.
- Ilinich, O. M.; Zamarev, K. J. *J. Membr. Sci.* **1993**, *82*, 149.
- Gajbhiye, S. B. *J. Appl. Polym. Sci.* **2013**, *127*, 2497.
- Khotimskii, V. S.; Filippova, V. G.; Bryantseva, I. S.; Bondar, V. I.; Shantarovich, V. P.; Yampolskii, Y. P. *J. Appl. Polym. Sci.* **2000**, *78*, 1612.
- Madkour, M. *Polymer* **2000**, *41*, 7489.
- Dai, Y.; Guiver, M. D.; Robertson, G. P.; Bilodeau, F.; Kang, Y. S.; Lee, K. J.; Jho, J. Y.; Won, J. *Polymer* **2002**, *43*, 5369.
- Lee, K. J.; Jho, J. Y.; Kang, Y. S.; Dai, Y.; Robertson, G. P.; Guiver, M. D.; Won, J. *J. Membr. Sci.* **2003**, *212*, 147.
- Vankrevelen, D. W. Properties of Polymers: Their Correlation with Chemical Structure, 3rd ed.; Elsevier: Amsterdam, **1990**.
- Crank, J. Mathematics of Diffusion; Oxford University Press: London, **1975**.
- Hernandez, R. J.; Gavara, R. *J. Polym. Sci. Part B: Polym. Phys.* **1994**, *32*, 2367.
- Silverstein, R. B.; Bassler, G. C.; Morrill, T. C. Spectrometric Identification of Organic Compounds, 2nd ed.; Wiley: New York, **1991**.
- Campanelli, A. R.; Domenicano, A.; Ramondo, F.; Hargittai, I. *Struct. Chem.* **2011**, *22*, 361.
- Semenova, S. L. *J. Membr. Sci.* **2004**, *231*, 189.
- Pace, R. J.; Dadyner, A. *J. Polym. Sci.* **1979**, *17*, 437.
- Ilinich, O. M.; Lapkin, A. A. *Polymer* **2002**, *43*, 3209.